

JGR Biogeosciences



RESEARCH ARTICLE

10.1029/2023JG007463

Key Points:

- Methane (CH₄) formation rates in lake sediment varied greatly among nine Swedish lakes located in different biogeographic regions
- CH₄ formation rates are related to reactivity and quantity of organic matter in the sediment, primarily to sediment age and total nitrogen
- CH₄ formation rates measured in contrasting sediment, spanning from Amazonia to Arctic tundra could be predicted by a common empirical model

Supporting Information:

Supporting Information may be found in the online version of this article.

Correspondence to:

S. Moras,
simone.moras@ebc.uu.se

Citation:

Moras, S., Zellmer, U. R., Hiltunen, E., Grasset, C., & Sobek, S. (2024). Predicting methane formation rates of freshwater sediments in different biogeographic regions. *Journal of Geophysical Research: Biogeosciences*, 129, e2023JG007463. <https://doi.org/10.1029/2023JG007463>

Received 6 MAR 2023

Accepted 2 JAN 2024




Author Contributions:

Conceptualization: Simone Moras, Ursula Ronja Zellmer, Evelina Hiltunen, Charlotte Grasset, Sebastian Sobek
Data curation: Simone Moras, Ursula Ronja Zellmer, Evelina Hiltunen
Formal analysis: Simone Moras
Funding acquisition: Simone Moras, Sebastian Sobek
Investigation: Simone Moras, Ursula Ronja Zellmer, Evelina Hiltunen
Methodology: Simone Moras, Ursula Ronja Zellmer, Evelina Hiltunen, Charlotte Grasset, Sebastian Sobek

© 2024. The Authors.

This is an open access article under the terms of the [Creative Commons Attribution License](#), which permits use, distribution and reproduction in any medium, provided the original work is properly cited.

Predicting Methane Formation Rates of Freshwater Sediments in Different Biogeographic Regions

Simone Moras¹ , Ursula Ronja Zellmer¹, Evelina Hiltunen¹, Charlotte Grasset¹ , and Sebastian Sobek¹ 

¹Department of Ecology and Genetics, Uppsala University, Uppsala, Sweden

Abstract Freshwater lakes and reservoirs cover a small fraction of the Earth, however their emission of the greenhouse gas methane (CH₄) from the sediment to the atmosphere is disproportionately high. Currently, there is still a limited understanding of the links between sediment characteristics and CH₄ formation. Earlier studies have indicated that sediment age and nitrogen content are related to sediment CH₄ formation rates, but it is uncertain such relationships are valid across gradients of sediment characteristics. We therefore measured potential CH₄ formation rates in multiple layers of sediment sampled from nine lakes situated in the temperate, boreal and alpine biogeographic regions of Sweden, thus differing in productivity, catchment and climate properties. Potential CH₄ formation varied over 3 orders of magnitude, and was broadly related to the quantity and reactivity of organic matter, and generally decreased with sediment depth. Sediment age and total nitrogen content were found to be the key controlling factors of potential CH₄ formation rates, together explaining 62% of its variability. Moreover, the model developed from the Swedish lake sediment data was able to successfully predict the potential CH₄ formation rates in reservoirs situated in different biogeographic regions of Brazil ($R^2 = 0.62$). Therefore, potential CH₄ formation rates in sediments of highly contrasting lakes and reservoirs, from Amazonia to alpine tundra, could be accurately predicted using one common model (RMSE = 1.6 in ln-units). Our model provides a valuable tool to improve estimates of CH₄ emission from lakes and reservoirs, and illustrates the fundamental regulation of microbial CH₄ formation by organic matter characteristics.

Plain Language Summary Lakes and reservoirs are important emitters of methane, a strong greenhouse gas, to the atmosphere. Methane is produced in absence of oxygen by specific microbes that degrade the organic matter in the sediment. Currently, it is still uncertain which specific sediment properties control the production of methane, and if such properties are the same across lakes and reservoirs located in different ecosystem. To test this, we collected sediment cores from several lakes across different ecosystems in Sweden, and we measured potential methane formation rates. Methane formation rates varied greatly among lakes and was related to the quality and quantity of organic matter in the sediment. From this experiment, we calculated an empirical model that can predict methane formation rates as a function of sediment age and nitrogen content. Moreover, we found that our model could well predict potential methane formation rates in tropical reservoirs. In conclusion, sediment age and nitrogen content are universal controlling factors of methane formation rates across lakes and reservoirs in different ecosystems, from tropics to arctic tundra. Our findings provide a valuable tool to improve estimates of methane emission from lakes and reservoirs and illustrates how sediment characteristics play a crucial role in regulating methane formation rates.

1. Introduction

Inland waters are a major component of the global carbon (C) cycle by emitting C to the atmosphere and burying C into the sediment, even though they cover only 4% of the Earth surface (Cole et al., 2007; Tranvik et al., 2009). In particular, inland waters are a prominent source of carbon dioxide (CO₂) and methane (CH₄) to the atmosphere (Raymond et al., 2013; Saunois et al., 2020). Despite CH₄ emissions being lower than CO₂, CH₄ has a much higher global warming potential ($\sim 27 \pm 11$ on a 100 years-time scale; Forster et al., 2021) making it a critical component of Earth's climate. Better understanding what regulates CH₄ flux from inland waters is therefore of vital importance to assess the feedback of inland waters on climate (Aben et al., 2017).

Freshwater sediments are favorable environments for methanogenesis. CH₄ is formed during organic matter decomposition in anoxic sediment, even though recent studies have shown that CH₄ can also be formed in oxygenated water columns (Günthel et al., 2019). Methanogenesis is favored when alternative electron acceptors (e.g.,

Project Administration: Sebastian Sobek

Sobek

Resources: Sebastian Sobek

Supervision: Sebastian Sobek

Visualization: Simone Moras

Writing – original draft: Simone Moras

Writing – review & editing: Simone

Moras, Ursula Ronja Zellmer, Evelina

Hiltunen, Charlotte Grasset, Sebastian

Sobek

Fe^{3+} , Mn^{4+} , NO_3^- , SO_4^{2-}) are depleted (Bastviken, 2009). A fraction of the CH_4 produced in the sediment is used for energy by methane oxidizing bacteria (King, 1992), while the rest reaches the atmosphere through three major pathways: diffusion, transport through the stems of emergent aquatic plants and ebullition (Bastviken, 2009). Compared to diffusion and plant-mediated fluxes, ebullition fluxes are generally considered the major component of total CH_4 emission from lakes and reservoirs (Bastviken, 2009; Deemer et al., 2016), because the very low solubility of CH_4 in water facilitates the formation of bubbles in sediment. However, CH_4 ebullition is highly heterogeneous across space and time (DeSontro et al., 2011; Linkhorst et al., 2020; Maeck et al., 2013; Mattson & Likens, 1990) and thus difficult to measure representatively. Models that incorporate the fundamental processes governing CH_4 production and transport constitute an alternative approach to estimate CH_4 ebullition at larger spatial and temporal scales.

Previous studies have shown a positive exponential relationship between methanogenesis and temperature in freshwater sediment (Duc et al., 2010; Yvon-Durocher et al., 2014). Less straightforward, however, are the links between CH_4 production and sediment characteristics. Studies have shown that CH_4 formation (i.e., production minus anaerobic oxidation) in freshwater sediments is related to organic matter supply and lability (Grasset et al., 2018; Schwarz et al., 2008; West et al., 2012), grain size (Bodmer et al., 2020) and sediment depth (Wilkinson et al., 2015). This limited understanding between CH_4 formation and sediment characteristics is reflected also in the mathematical models describing CH_4 fluxes from lakes to the atmosphere. Temperature and hydrodynamics are well incorporated in such models (Delwiche et al., 2022; Mogollón et al., 2012; Prairie et al., 2017; Stepanenko et al., 2016; Tan et al., 2015) while sediment characteristics are estimated or calibrated. An empirical CH_4 formation model developed by Isidorova et al. (2019a) showed that methane formation can be predicted from sediment age and nitrogen content. This model, however, was developed by incubating sediment of three tropical reservoirs in Brazil. It is unclear, therefore, if it can be applied for sediment of other lake ecosystems in other biogeographic regions, and if sediment age and nitrogen content are robust CH_4 formation predictors across a wider range of lake ecosystems and thus sediment properties. Here, we developed a CH_4 formation model for sediments from nine Swedish lakes differing in productivity, catchment area and climate. The aims of this study were (a) identifying the sediment characteristics that have a major effect on CH_4 formation and (b) testing whether a general CH_4 formation model could be developed for predicting sediment potential CH_4 formation across a wide range of sediment characteristics found in lakes of different productivities and situated in different biogeographic regions. We hypothesized that sediment age and total nitrogen can predict potential CH_4 formation rates in different types of sediments of Northern lakes and therefore they can be used as universal predictor of methane formation rates from lake sediments.

2. Materials and Methods

2.1. Sediment Sampling

Sediment cores from the pelagic area of nine Swedish lakes were sampled to measure potential CH_4 formation rates (Figure 1). The sampling strategy of this study was to acquire very different kinds of lake sediments, in order to address the hypothesis. The sampled sediment cores should not be regarded as representative for the respective lake basin, and the results are not representative for each lake, but specific to the sediment core sampled from that lake. The sampled lakes are located at different latitudes, differing in area, nutrient content, land use and climate, in order to cover wide ranges of sediment characteristics. Four lakes are located in the temperate forest biogeographic region of southern Sweden (Alstasjö, Ekoln, Gundlebosjön and Stora Galten) in the climatic region Dfb (warm-summer humid continental climate) according to Köppen-Geiger classification (Beck et al., 2018). Three of these lakes (Alstasjö, Ekoln and Gundlebosjön) are eutrophic ($\text{TP} > 25 \mu\text{g L}^{-1}$), while Stora Galten is oligotrophic ($\text{TP} < 10 \mu\text{g L}^{-1}$). This group of lakes will be defined as “temperate lakes” in the rest of the paper.

Two lakes are situated in the boreal forest biogeographic region of northern Sweden (Nedre Björntjärn and Nästjärn), located in the climatic zone Dfc (subarctic climate) and both lakes are dystrophic due to high concentration of dissolved humic matter. Three lakes (Bodsjön, Gevsjön and Norra Sandtjärn) are located in the alpine tundra biogeographic region of the Scandinavian mountains, and can be classified as oligotrophic ($\text{TP} < 10 \mu\text{g L}^{-1}$). Despite these lakes being located in the same climatic zone as the boreal lakes we considered them as “alpine lakes” since the markedly different characteristics of their catchments, where heathland above the tree line, a landscape typical of mountainous regions, is predominant while it is absent in our sampled boreal lakes. An

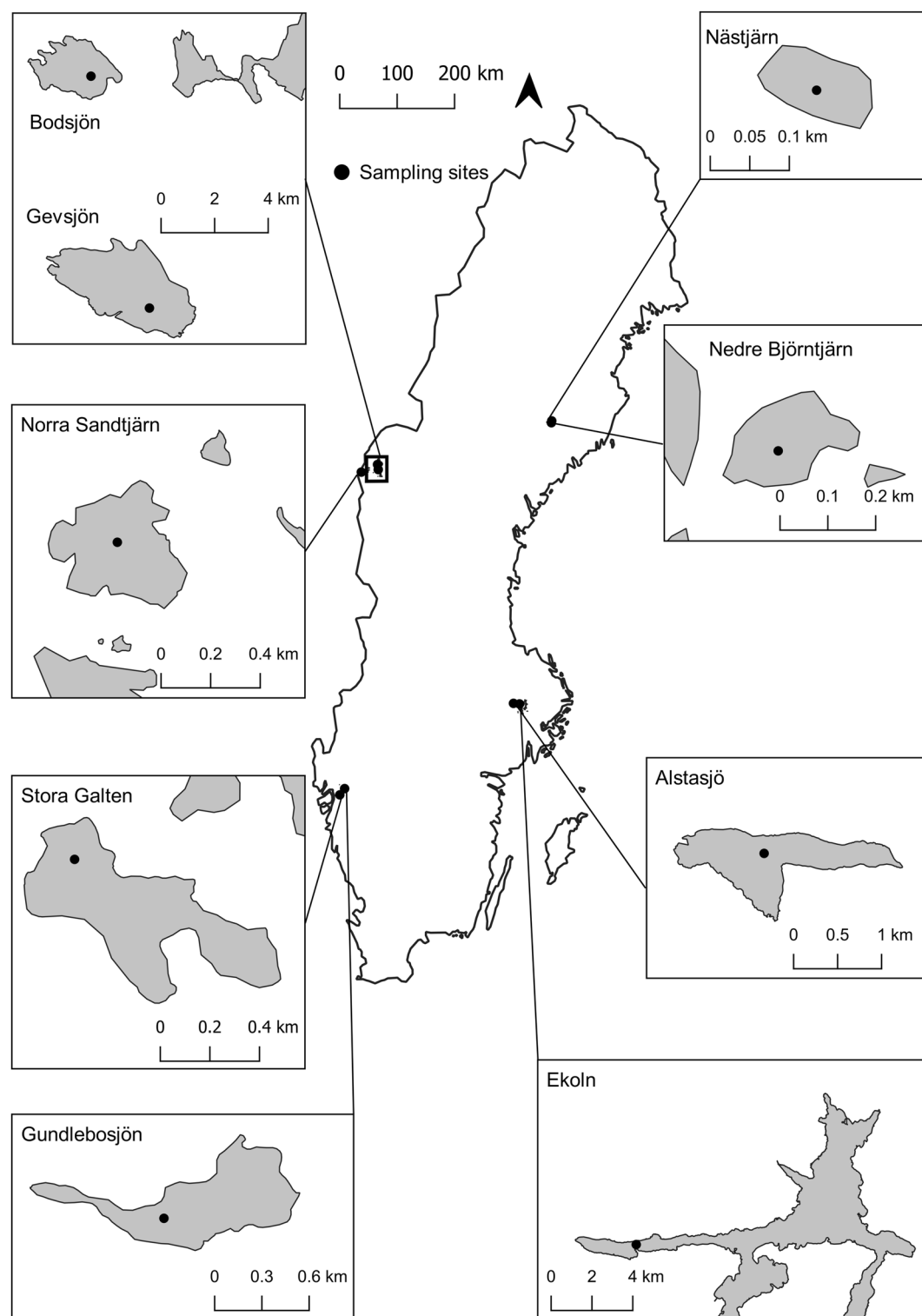


Figure 1. Overview of the lakes location and sediment sampling points (Bodsjön 63°26'56.1" N, 12°37'56.9"E; Gevsjön 63°22'13.3"N, 12°40'02.4"E; Norra Sandtjärn 63°18'55.1"N, 12°04'58.4"E; Nästjärn 64°09'01.1"N, 18°47'60.0"E; Nedre Björntjärn 64°07'18.8"N 18°47'04.3"E; Stora Galten 58°14'46.5"N 12°02'18.0"E; Gundlebosjön 58°20'54.4"N 12°10'12.5"E; Alstasjö 59°44'36.2"N 17°15'09.5"E; Ekoln 59°43'57.7"N 17°26'23.4"E).

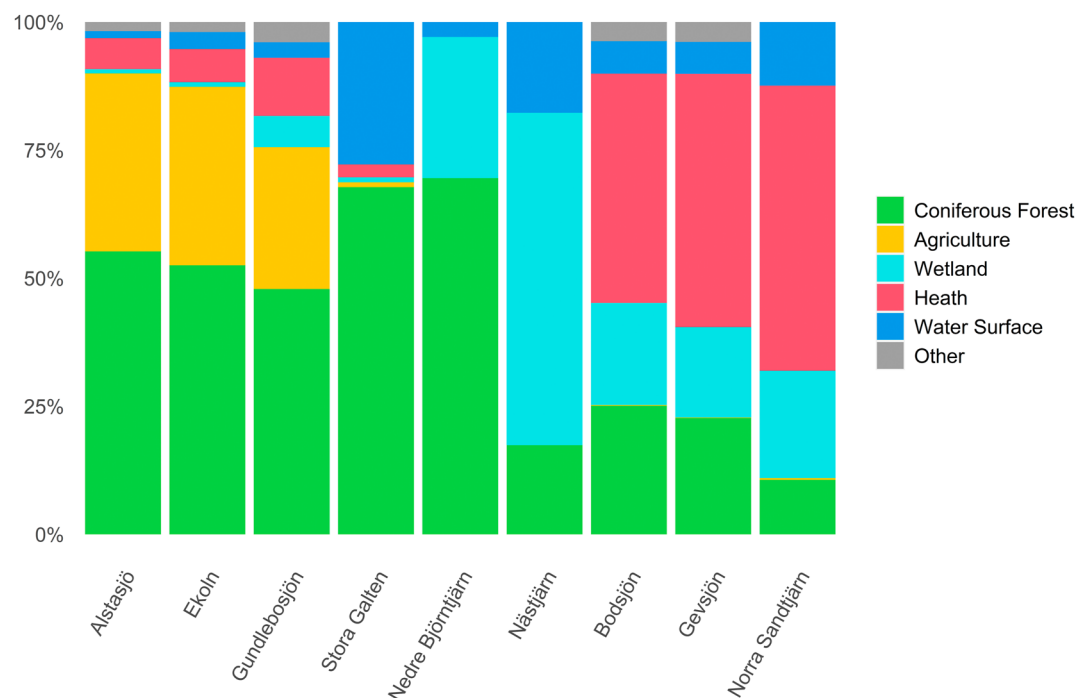


Figure 2. Land use of the catchment area of the sampled lakes in this study. Alstasjö, Ekoln Gundlebosjön, and Stora Galten are located in the temperate forest biogeographic region, Nedre Björntjärn and Nästjärn are located in the boreal forest biogeographic region, and Bodsjön, Gevsjön, and Norra Sandtjärn are located in the alpine tundra biogeographic region.

overview of catchment land use of the sampled lakes is found in Figure 2 and a summary of lake characteristics can be found in Table 1, while climatic data for each lake are available in Supporting Information S1 (Table S1).

Three sediment cores were taken at the deepest point of each lake using a UWITEC gravity core sampler (UWITEC, Mondsee, Austria) using 60 cm long PVC tubes between August 2019 and July 2020. One sediment core for each lake was used for incubation, one for estimating sediment age and the third one for sediment analysis. Sediment cores (length between 7 and 36 cm) were stored in the PVC tubes in dark condition at 4°C until analysis. Water samples for analysis of dissolved total nitrogen (Tot N), total phosphorus (Tot P), dissolved organic carbon (DOC) and pH were taken in lakes in which information from other sources was not available (see Table 1). Total nitrogen and total phosphorus concentration were measured with a UV/V spectrophotometer (Lambda 40; Perkin

Table 1
Physical and Chemical Properties of the Sampled Lakes

Lake	Lake area (km ²)	Catchment area (km ²)	Max depth (m)	Tot N (μg L ⁻¹)	Tot P (μg L ⁻¹)	DOC (mg L ⁻¹)	pH
Alstasjö (Temperate, Eutrophic)	1.28 ^a	707.7 ^a	4 ^a	1,060 ^b	147 ^c	21 ^c	8.1 ^c
Ekoln (Temperate, Eutrophic)	21.5 ^a	3,363 ^a	40 ^a	1,167 ^b	31 ^b	12 ^b	8 ^c
Gundlebosjön (Temperate, Eutrophic)	0.43 ^d	16.9 ^d	12 ^c	615 ^c	30 ^b	17 ^c	7 ^b
Stora Galten (Temperate, Oligotrophic)	0.31 ^d	1.1 ^d	22 ^c	180 ^c	4 ^b	4 ^c	6.8 ^b
Nedre Björntjärn (Boreal, Dystrophic)	0.03 ^d	3.5 ^d	10 ^c	564 ^c	22 ^c	18.2 ^f	5.6 ^e
Nästjärn (Boreal, Dystrophic)	0.05 ^d	0.03 ^d	10 ^c	687 ^c	21 ^c	9 ^c	6.8 ^c
Bodsjön (Alpine, Oligotrophic)	5.3 ^a	2,139.1 ^a	5 ^a	156 ^a	4.4 ^c	—	5.3 ^c
Gevsjön (Alpine, Oligotrophic)	11.23 ^a	1,689.5 ^a	31.6 ^a	155 ^a	4.3 ^c	—	5.5 ^c
Norra Sandtjärn (Alpine, Oligotrophic)	0.35 ^d	2.82 ^d	9 ^c	—	6.5 ^c	—	4.7 ^c

Note. In brackets are shown the biogeographic region and the trophic status of each lake. Data sources:

^a<http://vattenweb.smhi.se/modelarea/>. ^b<https://miljodata.slu.se/MVM>. ^cOwn measurement. ^dQGIS 3.22 analysis results (QGIS Development Team, 2009). ^eGustav Pajala personal communication. ^fSobek et al. (2003).

Elmer; Waltham, Massachusetts, USA). Total nitrogen was measured at two wavelengths (220 and 275 nm) and EDTA was used as calibration solution (Franson, 1976), while total phosphorus was measured at 882 nm using the molybdenum-blue method (Menzel & Corwin, 1965). A TOC/TN analyzer (Shimadzu TOC-L/TNM-L, Kyoto, Japan) was used to determine dissolved organic carbon in filtered lake water (filter pore size 0.7 μm). pH was measured using a pH-meter (Philips PW9420).

2.2. Sediment Incubation

Six sediment layers at different depths were incubated from each lake to assess changes in methane production rates with sediment depth. One sediment core from each site was sliced into 1 cm layers, except alpine lakes, for which cores were sliced into 0.5 cm layers since we assumed a low sedimentation rate. For each core, the first, second and fourth layer (counting from the top of the core) were selected for incubation, while the other three layers were distributed evenly over the remaining length of the sediment core. We considered the sediment layers within the first 4 cm to be “shallow layers” while deeper layers were regarded as “deep layers.”

The sediment of each layer was distributed into triplicate 60 glass vials, and 2.5–5 ml of water from the corresponding lake was added into the vials to create a sediment slurry. Water was pre-filtered through a 0.7 μm filter (Whatmann GF/F, Buckinghamshire, UK, filter unit: Millipore, Eschborn, Germany) to remove particulate organic matter. The vials were closed gas-tight with a 10 mm thick butyl rubber stopper and a crimp seal, leaving a headspace gas phase of ~ 52 mL. The headspace of each vial was then flushed with nitrogen gas for 15 min to create anoxic conditions within the vials. Sediment layers were incubated in dark conditions at 25°C in a temperature-controlled oven. Even though the temperature of incubation is higher than the natural sediment temperature of the sampled lakes, several studies in both wetlands and lakes have shown that an increase in sediment temperature up to 37–45°C do not significantly change the methanogenic microbial composition but only the microbial activity (Deng et al., 2019; Lavergne et al., 2021; Metje & Frenzel, 2005), therefore, in our experimental setups, unexpected results in potential CH_4 formation rates due to artificial warming are unlikely to occur.

To measure potential CH_4 formation, 5 ml of gas was taken at each sampling occasion from the headspace of each vial using a needle (0.5 \times 25 mm, BD Microlance 3, Drogheda, Ireland) and syringe to penetrate the rubber stopper of the vial. The syringe was equipped with a three-way stopcock that was open when taking the 5 mL of gas and closed before removing the needle from the bottle. In this way, the gas sample was never open to atmosphere, and thus no air could get sucked inside the syringe even if there was under pressure in the syringe. The vials were shaken before sampling in order to equilibrate the gas between the liquid phase (sediment slurry) and the gas phase in the vial. Headspace gas was injected into an Ultra-Portable Gas Analyzer (UGGA, Los Gatos Research, Mountain View, California, USA) using a custom-made discrete sample inlet port to measure CH_4 concentration. After each sampling occasion, 5 mL of N_2 were injected to the vials to avoid drops in pressure. Measurements were taken from day 7 since the start of incubation, and then every 3–4 days to monitor changes in CH_4 concentration within the vials. The incubation lasted 16–17 days. Since CH_4 concentrations were not negligible at the first measurement occasion in most lakes, we did not remove from our calculations any lag-phase between the start of the incubation and the start of CH_4 formation. We calculated the potential CH_4 formation rates as the increase of CH_4 in the vial divided by the number of days since the start of incubation, returning a conservative estimate of the cumulative CH_4 formation during the duration of the incubation. The reported rates presented in this study were normalized to sediment dry weight or carbon content.

2.3. Sediment Analyses

2.3.1. Water Content and pH

Sediment cores that were not used for incubation were used for analyzing water content, sediment age, grain size distribution, total organic carbon (OC), total nitrogen (TN), total organic matter (OM) content and pH. For these analyses, the sediment cores were sliced using the same procedure as for the sediment incubations. We determined the water content of each sediment layer by calculating the difference between wet and dry weight of the sediment layer. Before drying the sediment, pH was also measured for each layer with a lab pH-meter (Philips PW9420). Sediment layers were freeze-dried for 24–48 hr (Minifast 680, Edwards) with a drying pressure of 100 kPa.

2.3.2. Sediment Dating

To determine the age of the sediment layers, gamma spectroscopy (IAF-Radioökologie GmbH, Dresden, Germany) was used to measure the activity of ^{210}Pb , a natural radioisotope, and ^{137}Cs , an anthropogenic fission product. The half-life of ^{210}Pb is 22.3 years, so its activity constantly decreases with sediment age while highest fallout of ^{137}Cs was around 1963 (peak of nuclear weapons testing) and 1986 (Chernobyl accident). The sediment age was calculated from the unsupported ^{210}Pb activity using the constant rate of supply model (Appleby & Oldfield, 1978). Sediment accumulation rates for layers older than 120–150 years (these layers do not yield a ^{210}Pb activity anymore) were extrapolated to deeper layers to return indicative ages, by taking the average sediment accumulation rates of the layers younger than 120–150 years. When ^{210}Pb did not show the expected exponential decline over sediment depth, we used the ^{137}Cs peak to determine the age of sediment. The sediment layers with highest value of ^{137}Cs for each lake were assumed to be the Chernobyl accident in 1986. The sedimentation rate was calculated by dividing the depth of the sediment layers with the highest concentration of ^{137}Cs with the time between 1986 and the date of sampling. We assumed a constant sedimentation rate for sediment layers older than 1986.

2.3.3. Organic Carbon and Total Nitrogen

Around 100–200 mg of ground dried sediment from each layer was used to measure organic carbon (OC) and total nitrogen (TN) content using CS4010 CHNSO analyzer (Costech elemental combustion system, Valencia, USA). Sediment was acidified before analysis, by adding 100 μl of deionized water and 300–1,000 μl of 5% hydrochloric acid (HCl) to the sediment to remove inorganic carbon. Sediment layers from the boreal lakes were not acidified, since no inorganic carbon was found in a trial of subset of samples. The samples were dried overnight at 60°C before measurements. Triplicates of total C and total N were measured and the molar C:N ratio was calculated for each sediment layer.

2.3.4. Grain Size and Organic Matter

Around 1–2 g of each dried sediment layer was dry-ashed at 550°C for 4 hr to remove organic matter (OM) (loss on ignition method). The sediment samples were weighed before and after dry-ashing to quantify OM content. The dry-ashed sediment was then dispersed in 2 ml deionized water and sonicated for 5 min in an ultra-sound bath (Bandelin Sonorex Digitec, DT514BH-RC, Berlin, Germany) to disrupt particle aggregates. Grain size distribution of each sediment layer was measured using dynamic light scattering with a RF300 lens (MAM 5004, Malvern Master sizer, Worcestershire, United Kingdom). Each sample was measured at least five times to obtain consistent results.

2.4. Statistical Analyses

A Partial Least Squares (PLS) regression analysis was carried out to identify how far sediment characteristics (X variables) can explain potential CH_4 formation rates (Y variable). The potential CH_4 formation rates were expressed as $\mu\text{mol CH}_4 \text{ gDW}^{-1} \text{ d}^{-1}$, where DW stands for sediment dry weight. We did not normalize CH_4 by carbon (C) content to avoid having proxies of organic matter on both axes. Highly skewed variables were log-transformed prior to modeling. The variables were mean centered and scaled to unit variance. Model was validated with a permutation test by permuting 100 times the Y response variable. The X variables were ranked according their Variable Importance Projection (VIP, Eriksson et al., 2001). PLS analysis was carried out using SIMCA 17 (Umetrics, Umeå, Sweden). Differences in potential CH_4 formation rates along sediment depth and climatic regions were assessed using non-parametric Kruskal–Wallis test.

A linear regression model with interaction term was fitted between potential mass-specific CH_4 formation rates and the sediment characteristics that were identified as the most influential predictors from the PLS analysis. Model performance was checked visually by plotting residuals. To avoid multicollinearity, a Variance Inflation Factor analysis was carried out between independent variables in the linear regression analysis (Naimi et al., 2014). Even though a linear mixed effect model with “lake” as random effect could be a valuable alternative analysis in predicting potential mass-specific CH_4 formation rates, the resulting model cannot be applied to other lakes. The scope of this study is, on the other hand, to expand the applicability beyond our study sites. Therefore, we opted to choose a linear regression model.

In a second step, sediment potential mass-specific CH_4 formation rates measured in Brazilian reservoirs in Isidorova et al. (2019a) were fitted with the calculated linear regression model for our data in order to check if the model could well predict potential mass-specific CH_4 formation for sediments outside the studied lakes. To

Table 2
Sediment Characteristics of the Sampled Lakes

Lake	Water content (%)	OM (%)	OC (%)	TN (%)	C:N	Median grain size (μm)
Alstasjö (Temperate, Eutrophic)	77.2 (68.0–85.9)	12.7 (7.7–20.0)	3.4 (2.7–3.8)	0.4 (0.2–0.5)	11.3 (8.9–14.4)	5.9 (4.6–7.1)
Ekoln (Temperate, Eutrophic)	81.2 (74.0–89.4)	14.0 (6.3–20.0)	3.7 (3.0–4.3)	0.5 (0.4–0.5)	9.3 (8.6–9.8)	8.9 (2.6–18.7)
Gundlebosjön (Temperate, Eutrophic)	74.0 (61.0–85.5)	14.1 (7.7–17.6)	4.3 (3.0–5.0)	0.4 (0.3–0.5)	13.0 (11.1–14.6)	6.27 (2.8–12.1)
Stora Galten (Temperate, Oligotrophic)	93.6 (91.9–95.7)	44.1 (21.4–60.0)	18.1 (13.1–23.5)	0.9 (0.6–1.4)	22.2 (19.6–26.4)	25.2 (14.9–63.2)
Nedre Björntjärn (Boreal, Dystrophic)	96.1 (94.5–98.0)	85.5 (75–93.8)	43.9 (42.8–45.5)	2.4 (2.1–2.7)	21.5 (19.4–24.0)	11.0 (9.0–15.4)
Nästjärn (Boreal, Dystrophic)	95.8 (93.4–97.3)	72.0 (60.0–92.3)	40.2 (30.1–51.4)	2.9 (2.3–3.7)	15.9 (14.5–17.7)	12.9 (10.2–16.4)
Bodsjön (Alpine, Oligotrophic)	70.3 (65.9–73.2)	6.7 (6.3–7.2)	1.3 (1.1–1.8)	0.2 (0.1–0.3)	12.4 (9.4–13.9)	19.0 (13.8–25.0)
Gevsjön (Alpine, Oligotrophic)	56.0 (27.8–81.8)	6.4 (1.5–12.8)	1.8 (0.4–3.0)	0.2 (0.1–0.2)	10.0 (9.7–10.5)	25.4 (19.7–34.5)
Norra Sandtjärn (Alpine, Oligotrophic)	85.1 (83.3–86.9)	20.9 (6.3–30.6)	7.4 (6.4–9.0)	0.5 (0.4–0.6)	17.6 (15.5–20.3)	22.3 (12.5–38.3)

Note. In brackets are shown the biogeographic region and the trophic status of each lake. The numbers shown are core-averaged values and min and max value measured in the core (within round brackets).

render comparable data, we extracted and used the maximum potential mass-specific CH_4 formation rates from the data of Isidorova et al. (2019a). All analyses, excluding PLS, was carried out using R version 4.2.2 (R Core Team, 2022).

3. Results

3.1. Sediment Characteristics

Sediment characteristics showed a large variability among lakes (Table 2). The core-averaged OM content was much higher in the dystrophic boreal lakes (85.5% Nedre Björntjärn, 72.0% in Nästjärn) compared to the other lakes (range, 6.4%–44.1%). This resulted in correspondingly high OC and TN content (expressed as % of dry mass) in the boreal lakes (core-averaged TOC: 43.9% in Nedre Björntjärn, 40.2% in Nästjärn; core-averaged TN: 2.4% in Nedre Björntjärn, 2.9% in Nästjärn). High variability is shown also in C:N ratio with a minimum in Ekoln (core-average C:N ratio: 9.3) and a maximum in Stora Galten (core-average C:N ratio: 22.2).

Sedimentation rates varied greatly among lakes, with the highest sedimentation rates measured at the three eutrophic lakes while the other lakes showed much lower sedimentation rates which were then reflected in older age in the sampled sediment cores. A synthesis of activities of unsupported ^{210}Pb and ^{137}Cs and calculated sediment ages are provided in Supporting Information S1 (Tables S2–S10).

3.2. Potential CH_4 Formation Rates in Shallow and Deep Sediment

If normalizing potential CH_4 formation rates to sediment dry weight we found that the highest rates were measured in the organic-rich boreal lakes, for example, in the surface layer (depth 0–1 cm) Nästjärn ($9.9 \mu\text{mol CH}_4 \text{ gDW}^{-1} \text{ d}^{-1}$). However, when normalizing potential CH_4 formation rates by OC content, Alstasjö showed the highest formation rates in the surface layer ($37.0 \mu\text{mol CH}_4 \text{ gC}^{-1} \text{ d}^{-1}$). Overall, potential CH_4 formation rates in shallow layers (defined here as depth <4 cm) across lakes were significantly different from deep sediment layers (Kruskall-Wallis test, $p < 0.001$) except in the alpine lakes Bodsjön and Norra Sandtjärn, where potential CH_4 formation rates were extremely low in all the incubated layers, and differences in formation rates with depth were negligible (Figure 3, here shown as mass-specific potential CH_4 formation rates). Despite a strong decline in potential CH_4 formation rates toward deeper layers, CH_4 production never reached zero (Figure 3). As sediment depth was closely related to sediment age (see Tables S2–S10 in Supporting Information S1), the observed trends over depth corresponds to trends over age (Figure 4, here shown as mass-specific potential CH_4 formation rates). Accordingly, the highest potential CH_4 formation rates (in the lakes that show a marked decline with depth) were measured in the youngest sediment layer (i.e., 0–1 cm sediment layer depth), with the exception of lakes Ekoln and Gevsjön, where the highest rates were measured between 1 and 2 cm depth. The age of the layer 0–1 cm ranged from 0.6 years in Alstasjö to 43.2 in Bodsjön.

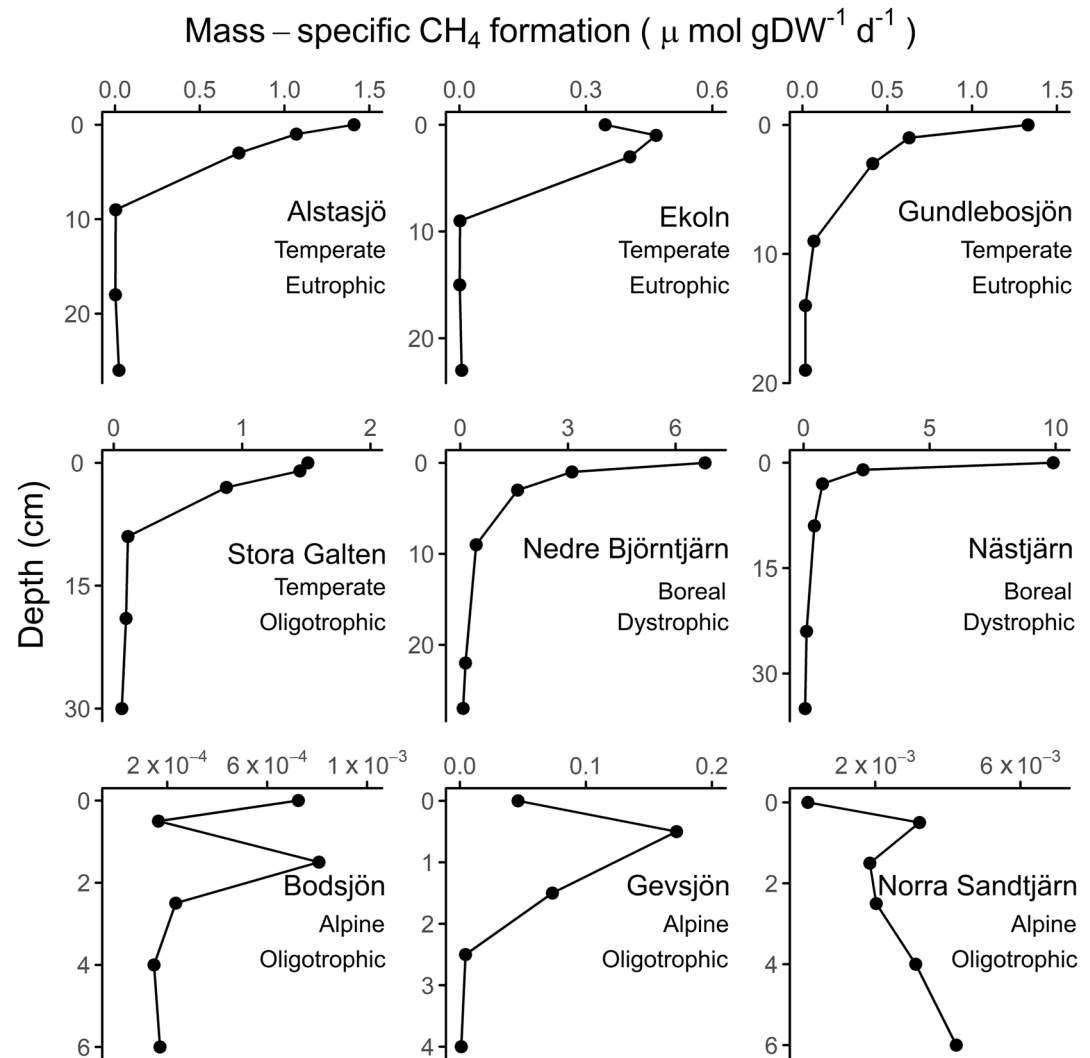


Figure 3. Potential mass-specific CH_4 formation rates over sediment depth. Lake name, biogeographic region and trophic status are also shown.

3.3. Potential CH_4 Formation Rates Across Biogeographic Regions and Trophic Status

Potential CH_4 formation rates in shallow layers (<4 cm sediment depth) significantly differed across biogeographic regions (Kruskal-Wallis test, $p < 0.001$). On average, the highest potential mass-specific CH_4 formation rates were measured in boreal lakes ($4.08 \pm 3.54 \mu\text{mol CH}_4 \text{ gDW}^{-1} \text{ d}^{-1}$), which are dystrophic and thus very rich in terrestrial organic matter. Potential mass-specific CH_4 formation rates in the temperate lakes were, on average, lower than in boreal lakes ($0.89 \pm 0.45 \mu\text{mol CH}_4 \text{ gDW}^{-1} \text{ d}^{-1}$). However, temperate lakes showed higher potential CH_4 formation rates when normalized by organic carbon content ($16.0 \pm 9.9 \mu\text{mol CH}_4 \text{ gC}^{-1} \text{ d}^{-1}$) than boreal lakes ($11.4 \pm 11.0 \mu\text{mol CH}_4 \text{ gC}^{-1} \text{ d}^{-1}$). Alpine lakes had much lower potential CH_4 formation rates ($0.02 \pm 0.04 \mu\text{mol CH}_4 \text{ gDW}^{-1} \text{ d}^{-1}$, $1.37 \pm 2.44 \mu\text{mol CH}_4 \text{ gC}^{-1} \text{ d}^{-1}$) in shallow sediment compared to boreal and temperate lakes. The same pattern across climatic regions was found in average potential mass-specific CH_4 formation rates in sediment layers deeper than 4 cm (boreal lakes: $0.2 \pm 0.1 \mu\text{mol CH}_4 \text{ gDW}^{-1} \text{ d}^{-1}$; temperate lakes: $0.03 \pm 0.03 \mu\text{mol CH}_4 \text{ gDW}^{-1} \text{ d}^{-1}$; alpine lakes: $0.002 \pm 0.0002 \mu\text{mol CH}_4 \text{ gDW}^{-1} \text{ d}^{-1}$), while temperate lakes did not show a higher potential CH_4 formation rates than boreal lakes when normalized by OC content (boreal lakes: $0.46 \pm 0.40 \mu\text{mol CH}_4 \text{ gC}^{-1} \text{ d}^{-1}$; temperate lakes: $0.45 \pm 0.44 \mu\text{mol CH}_4 \text{ gC}^{-1} \text{ d}^{-1}$; alpine lakes: $0.06 \pm 0.04 \mu\text{mol CH}_4 \text{ gC}^{-1} \text{ d}^{-1}$).

Potential mass-specific CH_4 formation rates differed also according to lake trophic status (Kruskal-Wallis test, $p < 0.01$). Dystrophic lakes showed the highest potential mass-specific CH_4 formation rates both in surface (4.0

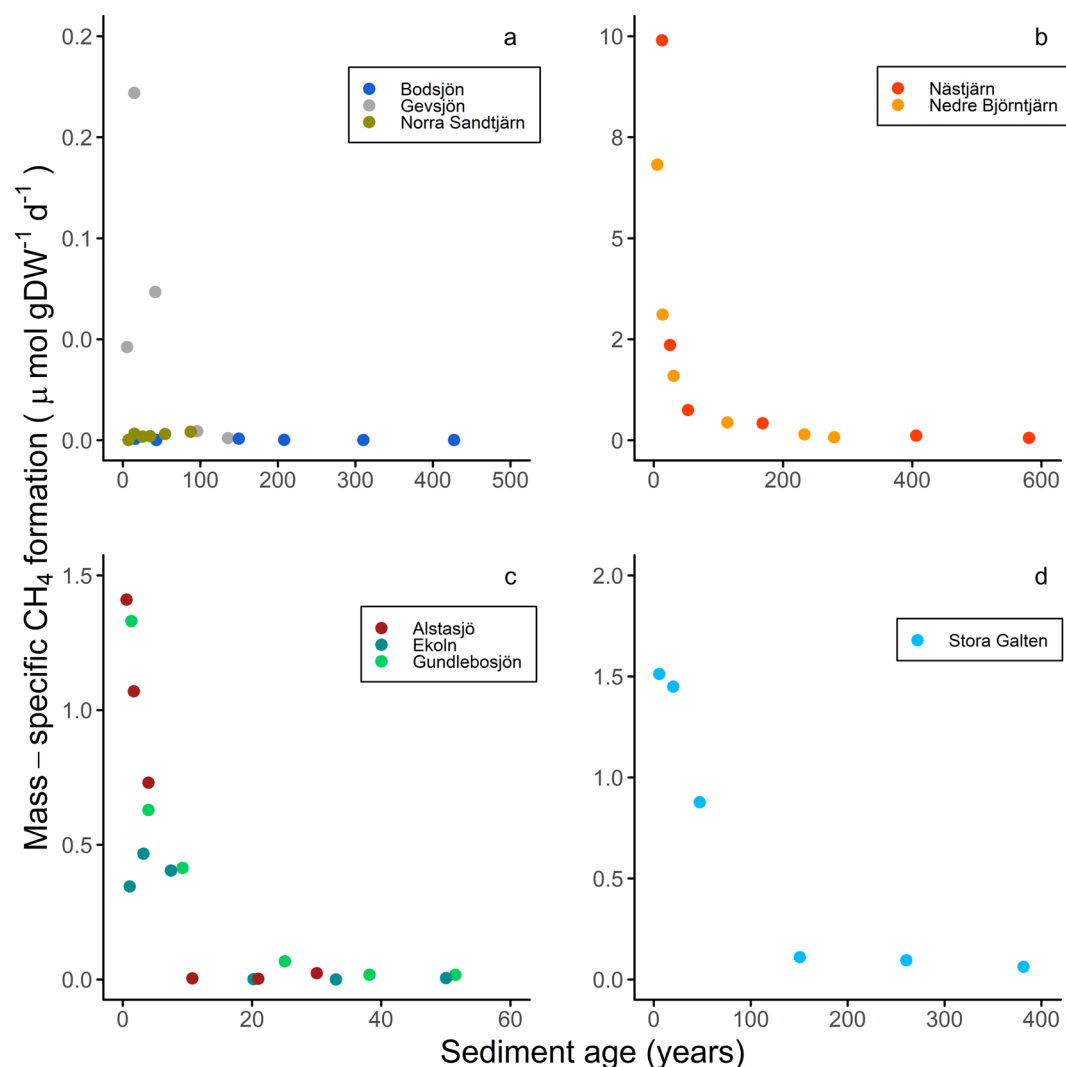


Figure 4. Potential mass-specific CH_4 formation rates in sediment over age in lake sediment. Lakes are grouped according to biogeographic regions (a = alpine lakes, b = boreal lakes, c = temperate lakes). Stora Galten (temperate lake) is displayed in panel (d) for better clarity, since the sediment age was higher than the other temperate lakes. Note the different magnitudes of the x and y scales. Ages >120–150 years are indicative ages derived from extrapolation of sediment accumulation rate from average sediment accumulation rates measured in the sediment layers younger than 150 years.

$8 \pm 3.54 \mu\text{mol CH}_4 \text{ gDW}^{-1} \text{ d}^{-1}$) and deep sediment ($0.21 \pm 0.17 \mu\text{mol CH}_4 \text{ gDW}^{-1} \text{ d}^{-1}$) compared to eutrophic ($0.76 \pm 0.41 \mu\text{mol CH}_4 \text{ gDW}^{-1} \text{ d}^{-1}$ for surface sediment; $0.02 \pm 0.02 \mu\text{mol CH}_4 \text{ gDW}^{-1} \text{ d}^{-1}$ for deep sediment) and oligotrophic lakes ($0.28 \pm 0.54 \mu\text{mol CH}_4 \text{ gDW}^{-1} \text{ d}^{-1}$ for surface sediment; $0.03 \pm 0.05 \mu\text{mol CH}_4 \text{ gDW}^{-1} \text{ d}^{-1}$ for deep sediment). Similarly, potential carbon-specific CH_4 formation rates varied significantly with lake productivity in surface sediment (Kruskal-Wallis test, $p < 0.001$) with highest rates in eutrophic lakes ($18.31 \pm 10.47 \mu\text{mol CH}_4 \text{ gC}^{-1} \text{ d}^{-1}$), followed by dystrophic lakes ($11.39 \pm 11.01 \mu\text{mol CH}_4 \text{ gC}^{-1} \text{ d}^{-1}$) and oligotrophic lakes ($2.90 \pm 4.01 \mu\text{mol CH}_4 \text{ gC}^{-1} \text{ d}^{-1}$). On the other hand, potential carbon-specific CH_4 formation rates in deep sediments did not differ significantly with lake productivity (average for all lakes: $0.36 \pm 0.41 \mu\text{mol CH}_4 \text{ gC}^{-1} \text{ d}^{-1}$).

3.4. Relationships Between Potential CH_4 Formation Rates and Sediment Characteristics

The PLS analysis extracted three significant components that explain 76% of the variance in potential mass-specific CH_4 formation rates ($R^2Y = 0.76$). Model validation through permutation analysis showed that background correlation was low ($R^2Y = 0.06$). The most important predictors of methane formation ($\text{VIP} > 1$) were TN, age, OM content, TC and pH of sediment (Figure 5). The loadings plot showed that potential mass-specific CH_4

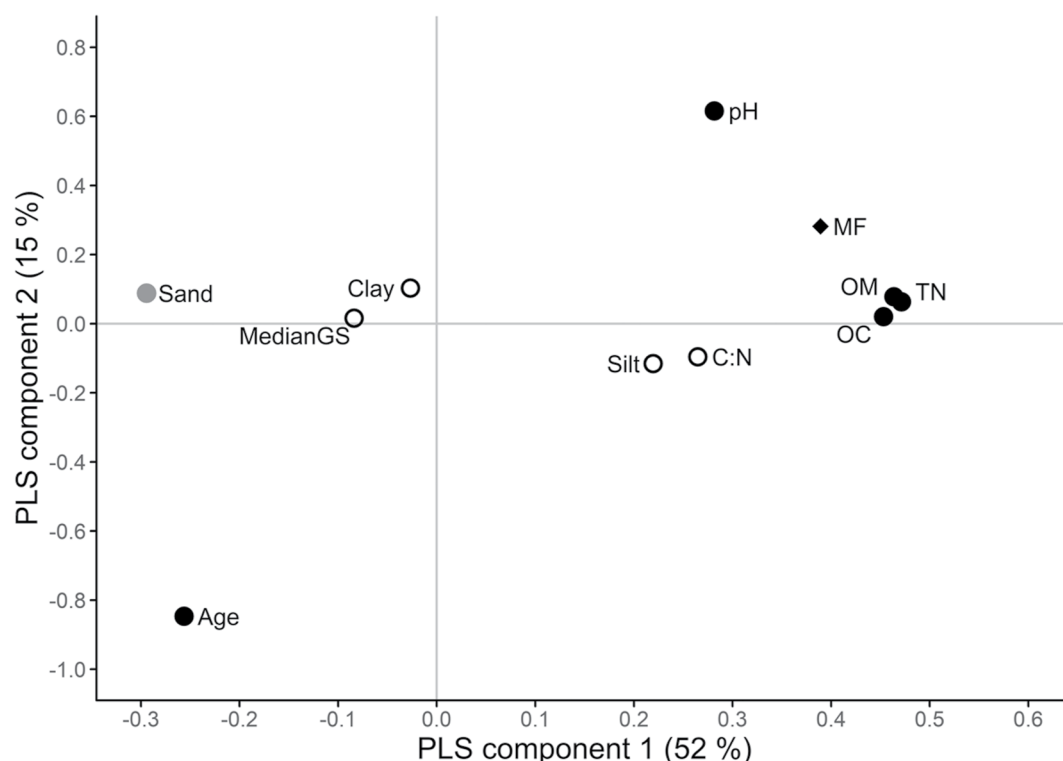


Figure 5. PLS loading plot between potential mass-specific CH_4 formation (MF) and sediment characteristics (OM = % organic matter; TN = % total nitrogen; OC = % organic carbon; MedianGS = Median grain size). Black dots show influential predictors ($\text{VIP} > 1$), gray dots show moderately influential predictors ($0.8 < \text{VIP} < 1$) and empty dots show less influential predictors ($\text{VIP} < 0.8$). X variables close to the Y variable are positively correlated, while X variable on the opposite side are negatively correlated.

formation rates were positively correlated with TN, OM, TC, and pH, while age was negatively correlated. Sand content was a moderately important predictor ($0.8 < \text{VIP} < 1$) and it was negatively correlated with potential mass-specific CH_4 formation rates. Sediment C:N ratio, silt, clay and median grain size were less influential predictors of potential mass-specific CH_4 formation rates ($\text{VIP} < 0.8$).

3.5. CH_4 Formation Model

Since the PLS analysis showed that the strongest predictors of potential mass-specific CH_4 formation rates were age and TN in our set of lake sediment, we fitted a linear regression model with these predictors into a single linear regression model. Collinearity of the predictors sediment age and TN was low ($R^2 = 0.21$; Variance inflation factor (VIF) was 1.1, well below the threshold of 10 that suggests collinearity concerns), which was also indicated in the PLS analysis (Figure 5) with age having a high loading on the vertical axis, and TN having a high loading on the horizontal axis. We did not include the other strong predictor variables from the PLS in our linear regression model to avoid multicollinearity, as TN, OM, and TC are strongly interrelated. pH was also an influential predictor of potential mass-specific CH_4 formation rates but was not included in the model for other reasons (see Section 4 for further details). The model revealed that age (years) and TN (mass %) could well predict potential mass-specific CH_4 formation rates (expressed as $\mu\text{mol gDW}^{-1} \text{d}^{-1}$) from our data set ($R^2 = 0.62$, $p < 0.001$) with no significant interaction term (Equation 1). Details on model statistics can be found in Supporting Information S1 (Table S11 in Supporting Information S1, for comparison, model performance with age and TN separately are also reported in Tables S12 and S13 of the Supporting Information S1).

$$\ln(\text{CH}_4 \text{ formation}) = -1.20 * \ln(\text{Age}) + 2.24 * \text{TN} - 1.19 \quad (1)$$

We then tested if the model developed for Brazilian reservoirs by Isidorova et al. (2019a) could predict potential mass-specific CH_4 formation rates of our data set, but the model did not perform very well for all our lakes

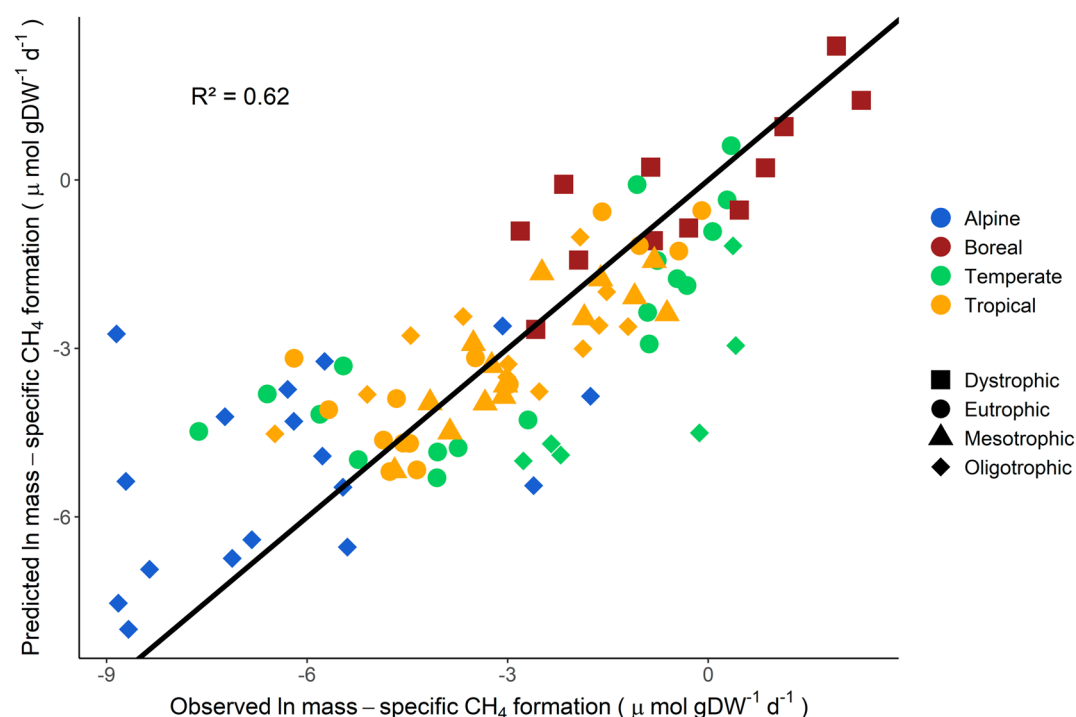


Figure 6. Observed versus predicted potential mass-specific CH_4 formation rates (in ln scale) in all sediment samples as a function of $\ln(\text{Age})$ and mass % of TN according to Equation 1. Note that potential CH_4 formation rates from Brazilian reservoirs in Isidorova et al. (2019a) were not used to build the model in the present study. The black line represents the 1:1 line. Lakes and reservoirs are grouped according to biogeographic region and trophic status.

($R^2 = 0.38$; not shown). Conversely, potential mass-specific CH_4 formation rates measured in the three tropical reservoirs in Isidorova et al. (2019a), which similarly to the Swedish lakes covered different biogeographic regions and ecosystem productivities, could be predicted well by the new model of the present study (Equation 1). The performance of the model for both Swedish lakes (this study) and Brazilian reservoirs (Isidorova et al., 2019a) is shown in Figure 6 ($R^2 = 0.62$, RMSE = 1.6 in ln-units).

4. Discussion

4.1. A Model of CH_4 Formation in Lakes and Reservoirs

This study shows that CH_4 formation in freshwater sediments can be predicted using one common model, across a wide range of ecosystem characteristics and climatic regions (Equation 1, Figure 6, $R^2 = 0.62$), and with a good degree of accuracy (RMSE = 1.6 in ln-units). Accordingly, the model performed well in predicting CH_4 from tropical reservoirs even though it was built on Swedish lakes. While this result may seem surprising given that the analyzed systems stretch from an Amazonian reservoir to alpine tundra lakes, it illustrates the fundamental regulation of CH_4 formation by sediment organic matter characteristics. Therefore, our model provides a valuable tool to estimate the methane formation potential in freshwaters across the world.

Our study also shows that age and nitrogen are universally important drivers of methane formation. We propose that sediment total nitrogen can be seen as a proxy of OM reactivity. N-rich compounds are rich in proteins that are preferentially consumed by microbes, reflected by a higher loss of TN in sediment over time compared to carbon (Gälman et al., 2008), thus reducing the reactivity of OM over time. The positive relationship of CH_4 formation and TN in sediment is in accordance with previous work carried out in rice-paddy soils (Yao et al., 1999), dredged river sediment (Gebert et al., 2006) and streams (Bodmer et al., 2020), highlighting TN as a strong driver of CH_4 formation across several different environments. In our study, TN was a better predictor of potential mass-specific CH_4 formation rates than the C:N ratio, which is often used as a proxy of OM quality (i.e., reactivity) (Duarte, 1992; Enríquez et al., 1993; Grasset et al., 2019). However, sediment TN incorporates both the OM reactivity, with high TN reflecting a high amount of protein-rich compounds, and the quantity of OM

in the sediment, with OM-rich sediment containing high amount of TN. Similarly, age can also be considered a proxy of OM reactivity. OM that settled onto the sediment a long time ago has been subjected to a longer period of degradation by microbes, thus reducing its reactivity compared to recently deposited sediment OM. The exponential relationship between organic carbon reactivity and age of sediment is well known for marine sediment (Middelburg et al., 1993) and is in accordance with our findings. Our model, therefore, describes how the OM originally deposited onto the sediment (quantity and quality indicator TN) and diagenetic change of OM after deposition (age) affects potential mass-specific CH_4 formation rates. The model presented in this study represents an expansion of a previous study (Isidorova et al., 2019a) and considerably broadens applicability to different lake and reservoir ecosystems.

The model presented here was able to predict potential mass-specific CH_4 formation rates across different ecosystems with an overall good level of accuracy ($\text{RMSE} = 1.6$), even though potential mass-specific CH_4 formation rates in some single layers with very low CH_4 formation (two layers in the alpine lakes Bodsjön and one layer in the alpine lake Norra Sandtjärn) were substantially overestimated by the model (residuals < -3 ln-units, Figure 6). We also note that potential mass-specific CH_4 formation rates from two sediment layers of the temperate lake Stora Galten was substantially underestimated by the model (residuals > 3 ln-units, Figure 6). Even though the model might occasionally predict erroneous potential mass-specific CH_4 formation rates of single sediment layers, we propose that it can be confidently applied at the scale of sediment columns or lake ecosystems, since errors in potential mass-specific CH_4 formation rates of individual sediment layers will average out with increasing number of predictions.

4.2. Highly Different Potential CH_4 Formation Rates Across Biogeographic Regions

The highest potential mass-specific CH_4 formation rates (expressed as $\mu\text{mol CH}_4 \text{ gDW}^{-1} \text{ d}^{-1}$) were measured in boreal lakes sediment. If compared to other lakes, boreal lakes sediment showed a higher C:N ratio (Table 2) reflecting a higher input of OM of terrestrial origin which has lower availability to microbial degradation compared to autochthonous OM (Grasset et al., 2021; Meyers & Ishiwatari, 1993; West et al., 2012). However, the much higher average OM content in boreal lakes (60%–93.8%; Table 2) compared to the alpine lakes (1.5%–30%; Table 2) and temperate lakes (6.3%–60%; Table 2) could explain why potential mass-specific CH_4 formation rates were highest in boreal lakes, congruent with reports of OM degradation rates being positively related to TN content (Enríquez et al., 1993) and OM addition (Grasset et al., 2018, 2021). Also, the colder climate in which boreal lakes are located compared to temperate lakes could partially explain why they have higher OM content in the sediment, as increasing temperature has a strong positive effect on OM mineralization (Gudas et al., 2010) and thus it can influence the sediment OM content.

The oligotrophic alpine lakes, on the other hand, despite being located in a similar climatic area and latitude as boreal lakes (mean annual temperature for alpine lakes: $2.1\text{--}2.9^\circ\text{C}$; mean annual temperature for boreal lakes: $2.5\text{--}2.7^\circ\text{C}$; see Table S1 in Supporting Information S1) showed very low potential CH_4 formation rates. In these lakes, sediment deposition rates were very low due to the low nutrient content in these lakes (Table 1) and so was the core-averaged TN content (Table 2). While the catchments of the studied boreal lakes are mostly dominated by forest and wetland, the catchment area of alpine lakes is mostly dominated by heathland (Figure 2), characterized by low vegetation and acidic soil. This could explain both the low input of OM onto the sediment and the low pH found in alpine lake sediment ($4.7\text{--}5.5$), which is known for limiting methanogenesis (Phelps & Zeikus, 1984). Accordingly, we found that pH was an important predictor and positively related to potential mass-specific CH_4 formation rates (Figure 5). Therefore, including pH into our linear regression model improved the model prediction of CH_4 formation ($R^2 = 0.66$, $p < 0.001$, Figure S1 in Supporting Information S1) compared to the original model using only age and TN as predictors (Equation 1; $R^2 = 0.62$). However, we chose not to incorporate pH in the final model (Equation 1) in order to make the model as widely useable as possible: pH is a parameter that must be measured in fresh sediment and shortly after sampling, and is not routinely measured in sediments, while age and TN can be measured in dry sediment, and thus data for prediction can be gained long after sediment sampling. In the purpose to make the model as widely applicable as possible, we opted to not use pH as predictor in our model. For comparison, model equation and performance including pH as predictor variable is available in Supporting Information S1 (Figure S1, Table S14).

Potential mass-specific CH_4 formation rates (i.e., expressed per sediment dry weight) in temperate lakes sediment were on average lower compared to boreal lakes (Figures 3 and 4). However, when normalizing potential

CH₄ formation rates by sediment carbon content, temperate lakes showed, on average, the highest potential carbon-specific CH₄ formation rates in the uppermost layers (depth < 4 cm, $16.0 \pm 9.9 \mu\text{mol CH}_4 \text{ gC}^{-1} \text{ d}^{-1}$). Apparently, the organic matter of sediments in the temperate lakes was more efficiently converted to methane, compared to alpine and boreal lakes. The lower C:N ratio in the temperate lakes (except oligotrophic Stora Galten) compared to the boreal lakes (Table 2) indicates a higher share of autochthonous OM, which is more available for methanogens (Grasset et al., 2018, 2019; West et al., 2012). In three of the four temperate lakes (with the exception of Stora Galten), a relevant share of the catchment area is covered by agricultural land (Figure 2) which causes higher nutrient input and primary production, a thus a higher supply of readily degradable autochthonous OM to the sediment. This finding provides mechanistic underpinning to reports of eutrophication triggering methane emission from lakes and reservoirs (Davidson et al., 2018; Deemer et al., 2016; Grasset et al., 2020).

Temperate Swedish lakes showed also similar potential mass-specific CH₄ formation rates patterns if compared to tropical reservoirs. Three of the four lake in the temperate area showed similar TC, TN, and C:N ratio to the Brazilian reservoirs (OM content was not available for the Brazilian reservoirs, refer to Table 1 in Isidorova et al. (2019a) and Table 2 in the present study). From the predicted versus observed potential mass-specific CH₄ formation rates (Figure 6) we can notice that sediment from the three tropical reservoirs, despite being characterized by highly different productivity (oligotrophic, mesotrophic and eutrophic; see Isidorova et al., 2019a) had more similar potential mass-specific CH₄ formation rates, while potential mass-specific CH₄ formation rates from Swedish lake sediments showed larger variability. It is also important to mention that potential mass-specific CH₄ formation rates in Isidorova et al. (2019a) measured in shallow sediment were taken from sub-surface (depth 2–6 cm) and did not account for the first two cm of sediment, possibly disregarding the highest potential mass-specific CH₄ formation rates in the sediment column and thus limiting overall data variability. Also, the fact that the Swedish data set was based on nine systems, as opposed to the three Brazilian systems, might relate to the higher variability in the Swedish data.

4.3. Potential CH₄ Formation Rates Decline With Depth and Age

Most lake sediments showed a steep decline in potential mass-specific CH₄ formation rates within the first 4 cm of sediment, with little CH₄ formation in the deepest layers (Figure 3). A decrease in CH₄ formation with sediment depth has been previously reported and it has been linked to a change in composition and an overall decrease in abundance in methanogenic microbes with depth and changes in methanogenic processes shifting from acetotrophic methanogenesis at the surface to hydrogenotrophic methanogenesis in deeper layers (Chan et al., 2005). Our sediment incubations of 0.5–1 cm thick layers of sediment provided an extremely high depth resolution in potential CH₄ formation rates, showing high variability in potential CH₄ formation over very small changes in depth. To our knowledge, this is the first study that measured potential CH₄ formation rates at this high depth resolution, providing new insights into the dynamics of CH₄ formation in lake sediments. We observe that CH₄ formation never reached zero even in very old (centuries) and deep sediment layers (Figures 3 and 4). Interestingly, the C:N ratio did not show a clear increase with depth for many of the studied lakes (Figure S2 in Supporting Information S1), nor did OM content, which increased with depth for several lakes (Figure S3 in Supporting Information S1), while there was no consistent trend in TN over depth for all lake sediments (Figure S4 in Supporting Information S1). To assess how potential CH₄ formation rates change with age (and corresponding depth), we fitted an exponential decay models for each lake sediment:

$$\text{CH}_4 = a * e^{-b * \text{Age}} + c \quad (2)$$

where CH₄ is the potential carbon-specific CH₄ formation rate ($\mu\text{mol/gC/d}$), a , b , and c are model parameters, Age is the age of the sediment (years). From these fits (Figures S5–S9, Table S15 in Supporting Information S1), we identified for each lake a transition age and depth in which the potential carbon-specific CH₄ formation rates can be considered negligible, defined as the point in which the slope of the decay model reached 179° (Isidorova et al., 2019a; see Supporting Information S1 for details). For some of the lakes, an exponential decay model could not be fit to the data because potential carbon-specific CH₄ formation rates were uniformly low over sediment depth (Bodsjön, Norra Sandtjärn) or did not follow an exponential decrease over age (Gevsjön, Ekoln) (Figures S10–S13 in Supporting Information S1).

The boreal lakes Nedre Björntjärn and Nästjärn showed a very similar transition age to negligible CH₄ formation at 54 and 58 years, respectively (Figures S5 and S6 in Supporting Information S1) and a corresponding transitional depth of about 5 cm. For the eutrophic temperate lakes Alstasjö and Gundlebosjö, the transition age was estimated at 30 years for both (Figures S7 and S8 in Supporting Information S1) and a corresponding transition

depth of about 26 and 12 cm respectively. The oligotrophic temperate lake Stora Galten showed the highest transitional age of around 150 years (Figure S9 in Supporting Information S1) and a corresponding to a transition depth of 10 cm. The eutrophic lakes had the youngest transition ages and also the highest sedimentation rates, in agreement with the positive relationship between sedimentation rate and carbon burial in freshwater (Sobek et al., 2009; Wilkinson et al., 2015) and marine sediment (Burdige, 2007). In fact, the three tropical reservoirs studied by Isidorova et al. (2019a) had on average 3 times higher sedimentation rates than the eutrophic Swedish lakes in the present study, and a transition age of only around 10 years (6.4–11.9 years corresponding to 9–23 cm depth). The overall lower transition age in the tropical reservoirs could also be explained by the high bottom water temperature (18–29°C) (Linkhorst et al., 2021; Quadra et al., 2020) triggering OM mineralization processes, particularly methanogenesis. The labile fraction of OM is therefore consumed more rapidly and the burial of OM that is recalcitrant to degradation occurs earlier. On the other hand, the boreal lakes in this study are ice-covered for about 5 months with an annual bottom water temperature close to 4°C, slowing down the speed of mineralization of labile OM and resulting in higher transition age.

These differences in transition ages across lakes show that it is not possible to relate significant potential carbon-specific CH_4 formation rates to sediment age and depth only. Even though some lakes in the same biogeographic region showed similar transition ages, our results suggest that making generalizations regarding at which sediment age potential carbon-specific CH_4 formation rates become negligible is not possible, presumably due to the influence of climate on the speed of OM mineralization rates and differences in sedimentation and OM supply rates.

4.4. Applicability of the Model to Streams and Rivers

PLS analysis showed that the strongest predictor of potential mass-specific CH_4 formation rates in lake sediment (with VIP > 1) were total nitrogen, age, OM content, OC content and pH (Figure 5). Sand content was a moderately influential parameter ($0.8 < \text{VIP} < 1$) while C:N ratio, median grain size, silt and clay content were less influential (VIP < 0.8).

Our results partially agree with a previous study on potential CH_4 formation rates on streams (Bodmer et al., 2020), which found that strong predictors of CH_4 formation were organic carbon and nitrogen content for secondary streams, while clay silt and organic carbon content were the strongest predictors for the main stream (in their study, nitrogen was not analyzed in the main stream). In addition, contrary to the stream sediments reported by Bodmer et al. (2020), we found that age was an important predictor of potential CH_4 formation rates in the studied lake sediments. The fact that age did not affect potential CH_4 formation rates in stream sediment might be related to the fact that sediments are much more mixed in streams than in lakes, such that depth gradients of OM characteristics (age and reactivity) cannot be expected to be very strong. Applying the model presented here (Equation 1) to lotic ecosystems such as streams and rivers, therefore, might not be appropriate, as the stronger sediment mixing in these environments can make sediment age difficult to estimate.

5. Implications

This study showed that sediment characteristics, namely age and total nitrogen are key controlling factors of maximum potential mass-specific CH_4 formation rates across a wide gradient of lake ecosystems and it represents a further step toward better estimates of CH_4 emission from inland waters. The present study, however, describes only some of the factors that regulate potential CH_4 formation rates and, consequently, CH_4 emission from freshwaters. CH_4 formation is also controlled by temperature (Jansen et al., 2022; Yvon-Durocher et al., 2014), OM supply rate (Grasset et al., 2021) and sediment oxygenation (Whiticar & Faber, 1986). Therefore, all these factors must be considered when modeling in situ potential CH_4 formation rates. Also, the obtained potential CH_4 formation rates should be corrected by in situ temperature (Yvon-Durocher et al., 2014, see Supporting Information S1) and could be coupled to physical models that describe gas dynamics in the sediment (Ramirez et al., 2015; Scandella et al., 2011) and in the water column (Stepanenko et al., 2016; Tan et al., 2015) to ultimately provide better estimate of CH_4 emission from freshwaters.

Data Availability Statement

Data and metadata are publicly available at Zenodo (Moras et al., 2023, <https://doi.org/10.5281/zenodo.8431310>). Data from Isidorova et al. (2019b) used in this study were retrieved from DIVA repository <http://uu.diva-portal.org/smash/record.jsf?pid=diva2%3A1329353&dswid=9967>. Lake characteristics and land use data of the

sampled lakes in this study were obtained from SMHI (Sveriges Meteorologiska och Hydrologiska Institut) Waterweb portal (SMHI & Havs och Vatten Myndigheten, 2022, <http://vattenweb.smhi.se/modelarea/>) and MVM (Miljödata-MVM, 2022, Mark, Vatten och Miljö data, for water chemistry <https://miljodata.slu.se/MVM>). Maps were created using QGIS version 3.22 (QGIS Development Team, 2009, <http://qgis.org>).

Acknowledgments

Financial support from the Swedish Research Council (VR, Grant 2017-04405) to S.S. and from the Olsson-Borgh and Malmén Foundations to S.M. is acknowledged. The authors are grateful to Gustav Pajala, José Paranaíba, and Henrique Sawakuchi for support during field campaigns and to Christoffer Bergvall and Mattias Lantz for support with sediment analyses.

References

- Aben, R. C. H., Barros, N., Van Donk, E., Frenken, T., Hilt, S., Kazanjian, G., et al. (2017). Cross continental increase in methane ebullition under climate change. *Nature Communications*, 8(1), 1–8. <https://doi.org/10.1038/s41467-017-01535-y>
- Appleby, P. G., & Oldfield, F. (1978). The calculation of lead-210 dates assuming a constant rate of supply of unsupported ^{210}Pb to the sediment. *Catena*, 5(1), 1–8. [https://doi.org/10.1016/S0341-8162\(78\)80002-2](https://doi.org/10.1016/S0341-8162(78)80002-2)
- Bastviken, D. (2009). Methane. In G. E. Likens (Ed.), *Encyclopedia of inland waters* (pp. 783–804). <https://doi.org/10.1016/B978-012370626-3.00117-4>
- Beck, H. E., Zimmermann, N. E., McVicar, T. R., Vergopolan, N., Berg, A., & Wood, E. F. (2018). Present and future Köppen-Geiger climate classification maps at 1-km resolution. *Scientific Data*, 5, 1–12. <https://doi.org/10.1038/sdata.2018.214>
- Bodmer, P., Wilkinson, J., & Lorke, A. (2020). Sediment properties drive spatial variability of potential methane production and oxidation in small streams. *Journal of Geophysical Research: Biogeosciences*, 125(1), e2019JG005213. <https://doi.org/10.1029/2019JG005213>
- Burdige, D. J. (2007). Preservation of organic matter in marine sediments: Controls, mechanisms, and an imbalance in sediment organic carbon budgets? *Chemical Reviews*, 107(2), 467–485. <https://doi.org/10.1021/cr050347q>
- Chan, O. C., Claus, P., Casper, P., Ulrich, A., Lueders, T., & Conrad, R. (2005). Vertical distribution of structure and function of the methanogenic archaeal community in Lake Dagow sediment. *Environmental Microbiology*, 7(8), 1139–1149. <https://doi.org/10.1111/j.1462-2920.2005.00790.x>
- Cole, J. J., Prairie, Y. T., Caraco, N. F., McDowell, W. H., Tranvik, L. J., Striegl, R. G., et al. (2007). Plumbing the global carbon cycle: Integrating inland waters into the terrestrial carbon budget. *Ecosystems*, 10(1), 171–184. <https://doi.org/10.1007/s10021-006-9013-8>
- Davidson, T. A., Audet, J., Jeppesen, E., Landkildehus, F., Lauridsen, T. L., Søndergaard, M., & Syväranta, J. (2018). Synergy between nutrients and warming enhances methane ebullition from experimental lakes. *Nature Climate Change*, 8(2), 156–160. <https://doi.org/10.1038/s41558-017-0063-z>
- Deemer, B. R., Harrison, J. A., Li, S., Beaulieu, J. J., DelSontro, T., Barros, N., et al. (2016). Greenhouse gas emissions from reservoir water surfaces: A new global synthesis. *BioScience*, 66(11), 949–964. <https://doi.org/10.1093/biosci/biw117>
- DelSontro, T., Kunz, M. J., Kempter, T., Wüest, A., Wehrli, B., & Senn, D. B. (2011). Spatial heterogeneity of methane ebullition in a large tropical reservoir. *Environmental Science and Technology*, 45(23), 9866–9873. <https://doi.org/10.1021/es2005545>
- Delwiche, K. B., Harrison, J. A., Maasakkers, J. D., Sulprizio, M. P., Worden, J., Jacob, D. J., & Sunderland, E. M. (2022). Estimating driver and pathways for hydroelectric reservoir methane emissions using a new mechanistic model. *Journal of Geophysical Research: Biogeosciences*, 127(8), 1–24. <https://doi.org/10.1029/2022JG006908>
- Deng, Y., Liu, P., & Conrad, R. (2019). Effect of temperature on the microbial community responsible for methane production in alkaline NamCo wetland soil. *Soil Biology and Biochemistry*, 132, 69–79. <https://doi.org/10.1016/j.soilbio.2019.01.024>
- Duarte, C. M. (1992). Nutrient concentration of aquatic plants: Patterns across species. *Limnology and Oceanography*, 37(4), 882–889. <https://doi.org/10.4319/lo.1992.37.4.0882>
- Duc, N. T., Crill, P., & Bastviken, D. (2010). Implications of temperature and sediment characteristics on methane formation and oxidation in lake sediments. *Biogeochemistry*, 100(1), 185–196. <https://doi.org/10.1007/s10533-010-9415-8>
- Enríquez, S., Duarte, C. M., & Sand-Jensen, K. (1993). Patterns in decomposition rates among photosynthetic organisms: The importance of detritus C:N:P content. *Oecologia*, 94(4), 457–471. <https://doi.org/10.1007/BF00566960>
- Eriksson, L., Johansson, E., Kettaneh-Wold, N., & Wold, S. (2001). *Multi-and megavariable data analysis: Principles and applications*. Umetrics AB.
- Forster, P., Storelvmo, T., Armour, K., Collins, W., Dufresne, J.-L., Frame, D., et al. (2021). The Earth's energy budget, climate feedbacks and climate sensitivity. In V. Masson-Delmotte, P. Zhai, A. Pirani, S. L. Connors, C. Péan, S. Berger, et al. (Eds.), *Climate change 2021: The physical science basis. Contribution of working group I to the sixth assessment report of the intergovernmental panel on climate change* (pp. 923–1054). <https://doi.org/10.1017/9781009157896.009.923>
- Franson, M. A. (1976). *Standard methods for the examination of water and wastewater*. American Public Health Association.
- Gälman, V., Rydberg, J., Sjöstedt de-Luna, S., Bindler, R., & Renberg, I. (2008). Carbon and nitrogen loss rates during aging of lake sediment: Changes over 27 years studied in varved lake sediment. *Limnology and Oceanography*, 53(3), 1076–1082. <https://doi.org/10.4319/lo.2008.53.3.1076>
- Gebert, J., Köthe, H., & Grönröft, A. (2006). Prognosis of methane formation by river sediments. *Journal of Soils and Sediments*, 6(2), 75–83. <https://doi.org/10.1065/jss2006.04.153>
- Grasset, C., Abril, G., Mendonça, R., Roland, F., & Sobek, S. (2019). The transformation of macrophyte-derived organic matter to methane relates to plant water and nutrient contents. *Limnology and Oceanography*, 64(4), 1737–1749. <https://doi.org/10.1002/lno.11148>
- Grasset, C., Mendonça, R., Villamor Saucedo, G., Bastviken, D., Roland, F., & Sobek, S. (2018). Large but variable methane production in anoxic freshwater sediment upon addition of allochthonous and autochthonous organic matter. *Limnology and Oceanography*, 63(4), 1488–1501. <https://doi.org/10.1002/lno.10786>
- Grasset, C., Moras, S., Isidorova, A., Couture, R. M., Linkhorst, A., & Sobek, S. (2021). An empirical model to predict methane production in inland water sediment from particular organic matter supply and reactivity. *Limnology and Oceanography*, 66(10), 3643–3655. <https://doi.org/10.1002/lno.11905>
- Grasset, C., Sobek, S., Scharnweber, K., Moras, S., Villwock, H., Andersson, S., et al. (2020). The CO₂-equivalent balance of freshwater ecosystems is non-linearly related to productivity. *Global Change Biology*, 26(10), 5705–5715. <https://doi.org/10.1111/gcb.15284>
- Gudas, C., Bastviken, D., Steger, K., Premke, K., Sobek, S., & Tranvik, L. J. (2010). Temperature-controlled organic carbon mineralization in lake sediments. *Nature*, 466(7305), 478–481. <https://doi.org/10.1038/nature09186>
- Günthel, M., Donis, D., Kirillin, G., Ionescu, D., Bizic, M., McGinnis, D. F., et al. (2019). Contribution of oxic methane production to surface methane emission in lakes and its global importance. *Nature Communications*, 10(1), 1–10. <https://doi.org/10.1038/s41467-019-13320-0>
- Isidorova, A., Grasset, C., Mendonça, R., & Sobek, S. (2019a). Methane formation in tropical reservoirs predicted from sediment age and nitrogen. *Scientific Reports*, 9(1), 1–9. <https://doi.org/10.1038/s41598-019-47346-7>
- Isidorova, A., Grasset, C., Mendonça, R., & Sobek, S. (2019b). Methane formation in tropical reservoirs predicted from sediment age and nitrogen [Dataset]. *Scientific Reports*, 9(1), 1–9. Retrieved from <http://uu.diva-portal.org/smash/record.jsf?pid=diva2%3A1329353&dsid=96>

- Jansen, J., Woolway, R. I., Kraemer, B. M., Albergel, C., Bastviken, D., Weyhenmeyer, G. A., et al. (2022). Global increase in methane production under future warming of lake bottom waters. *Global Change Biology*, 28(18), 5427–5440. <https://doi.org/10.1111/gcb.16298>
- King, G. M. (1992). Ecological aspects of methane oxidation, a key determinant of global methane dynamics. In K. C. Marshall (Ed.), *Advances in microbial ecology* (pp. 431–468). https://doi.org/10.1007/978-1-4684-7609-5_9
- Lavergne, C., Aguilar-Muñoz, P., Calle, N., Thalasso, F., Astorga-España, M. S., Sepulveda-Jauregui, A., et al. (2021). Temperature differently affected methanogenic pathways and microbial communities in sub-Antarctic freshwater ecosystems. *Environment International*, 154. <https://doi.org/10.1016/j.envint.2021.106575>
- Linkhorst, A., Hiller, C., DelSontro, T., Azevedo, G. M., Barros, N., Mendonça, R., & Sobek, S. (2020). Comparing methane ebullition variability across space and time in a Brazilian reservoir. *Limnology and Oceanography*, 65(7), 1623–1634. <https://doi.org/10.1002/lno.11410>
- Linkhorst, A., Paranaíba, J. R., Mendonça, R., Rudberg, D., DelSontro, T., Barros, N., & Sobek, S. (2021). Spatially resolved measurements in tropical reservoirs reveal elevated methane ebullition at river inflows and at high productivity global biogeochemical cycles. *Global Biogeochemical Cycles*, 35(5), 1–16. <https://doi.org/10.1029/2020GB006717>
- Maeck, A., Delsontro, T., McGinnis, D. F., Fischer, H., Flury, S., Schmidt, M., et al. (2013). Sediment trapping by dams creates methane emission hot spots. *Environmental Science and Technology*, 47(15), 8130–8137. <https://doi.org/10.1021/es4003907>
- Mattson, M. D., & Likens, G. E. (1990). Air pressure and methane fluxes. *Nature*, 347(5), 7198–7719. <https://doi.org/10.1038/347718b0>
- Menzel, D. W., & Corwin, N. (1965). The measurement of total phosphorus in seawater based on the liberation of organically bound fractions by persulfate oxidation. *Limnology and Oceanography*, 10(2), 280–282. <https://doi.org/10.4319/lno.1965.10.2.0280>
- Metje, M., & Frenzel, P. (2005). Effect of temperature on anaerobic ethanol oxidation and methanogenesis in acidic peat from a Northern Wetland. *Applied and Environmental Microbiology*, 71(12), 8191–8200. <https://doi.org/10.1128/AEM.71.12.8191-8200.2005>
- Meyers, P. A., & Ishiwatari, R. (1993). Lacustrine organic geochemistry—an overview of indicators of organic matter sources and diagenesis in lake sediments. *Organic Geochemistry*, 20(7), 867–900. [https://doi.org/10.1016/0146-6380\(93\)90100-P](https://doi.org/10.1016/0146-6380(93)90100-P)
- Middelburg, J. J., Vlug, T., Jaco, F., & van der Nat, W. A. (1993). Organic matter mineralization in marine systems. *Global and Planetary Change*, 8(1–2), 47–58. [https://doi.org/10.1016/0921-8181\(93\)90062-S](https://doi.org/10.1016/0921-8181(93)90062-S)
- Miljödata-MVM. (2022). Swedish University of Agricultural Sciences (SLU). National data host lakes and watercourses, and national data host agricultural land [Dataset]. Retrieved from <https://miljodata.slu.se/mvm/>
- Mogollón, J. M., Dale, A. W., Fossing, H., & Regnier, P. (2012). Timescales for the development of methanogenesis and free gas layers in recently-deposited sediments of Arkona Basin (Baltic Sea). *Biogeosciences*, 9(5), 1915–1933. <https://doi.org/10.5194/bg-9-1915-2012>
- Moras, S., Zellmer, U. R., Hiltunen, E., Grasset, C., & Sobek, S. (2023). Predicting methane formation rates of freshwater sediments in different biogeographic regions [Dataset]. <https://doi.org/10.5281/zenodo.8431310>
- Naimi, B., Hamm, N. A. S., Groen, T. A., Skidmore, A. K., & Toxopeus, A. G. (2014). Where is positional uncertainty a problem for species distribution modelling? *Ecography*, 37(2), 191–203. <https://doi.org/10.1111/j.1600-0587.2013.00205.x>
- Phelps, T. J., & Zeikus, J. G. (1984). Influence of pH on terminal carbon metabolism in anoxic sediments from a mildly acidic lake. *Applied and Environmental Microbiology*, 48(6), 1088–1095. <https://doi.org/10.1128/aem.48.6.1088-1095.1984>
- Prairie, Y. T., Alm, J., Harby, A., Mercier-Blais, S., & Nahas, R. (2017). The GHG Reservoir Tool (G-res) Technical documentation. Updated version 3.2 (2022-12-19). In *UNESCO/IHA research project on the GHG status of freshwater reservoirs*. Joint Publication of the UNESCO Chair in Global Environmental Change and the International Hydropower Association.
- QGIS Development Team. (2009). *QGIS geographic information system*. Open Source Geospatial Foundation. Retrieved from <http://qgis.org>
- Quadra, G. R., Sobek, S., Paranaíba, J. R., Isidorova, A., Roland, F., Do Vale, R., & Mendonça, R. (2020). High organic carbon burial but high potential for methane ebullition in the sediments of an Amazonian hydroelectric reservoir. *Biogeosciences*, 17(6), 1495–1505. <https://doi.org/10.5194/bg-17-1495-2020>
- Ramirez, J. A., Baird, A. J., Coulthard, T. J., & Waddington, J. M. (2015). Testing a simple model of gas bubble dynamics in porous media. *Water Resources Research*, 51(3), 1036–1049. <https://doi.org/10.1002/2014WR015898>
- Raymond, P. A., Hartmann, J., Lauerwald, R., Sobek, S., McDonald, C., Hoover, M., et al. (2013). Global carbon dioxide emissions from inland waters. *Nature*, 503(7476), 355–359. <https://doi.org/10.1038/nature12760>
- R Core Team. (2022). *R: A language and environment for statistical computing*. R Foundation for Statistical Computing. Retrieved from <https://www.R-project.org/>
- Saunois, M., Stavert, A. R., Poulter, B., Bousquet, P., Canadell, J. G., Jackson, R. B., et al. (2020). The global methane budget 2000–2017. *Earth System Science Data*, 12(3), 1561–1623. <https://doi.org/10.5194/essd-12-1561-2020>
- Scandella, B. P., Varadharajan, C., Hemond, H. F., Ruppel, C., & Juanes, R. (2011). A conduit dilation model of methane venting from lake sediments. *Geophysical Research Letters*, 38(6), 1–6. <https://doi.org/10.1029/2011GL046768>
- Schwarz, J. I. K., Eckert, W., & Conrad, R. (2008). Response of the methanogenic microbial community of a profundal lake sediment (Lake Kinneret, Israel) to algal deposition. *Limnology and Oceanography*, 53(1), 113–121. <https://doi.org/10.4319/lno.2008.53.1.0113>
- SMHI & Havs och Vatten Myndigheten. (2022). Modelldata per område [Dataset]. Retrieved from <https://vattenwebb.smhi.se/modelarea/>
- Sobek, S., Algesten, G., Bergström, A. K., Jansson, M., & Tranvik, L. J. (2003). The catchment and climate regulation of pCO₂ in boreal lakes. *Global Change Biology*, 9(4), 630–641. <https://doi.org/10.1046/j.1365-2486.2003.00619.x>
- Sobek, S., Durisch-Kaiser, E., Zurbrugg, R., Wongfun, N., Wessels, M., Pasche, N., & Wehrli, B. (2009). Organic carbon burial efficiency in lake sediments controlled by oxygen exposure time and sediment source. *Limnology and Oceanography*, 54(6), 2243–2254. <https://doi.org/10.4319/lno.2009.54.6.2243>
- Stepanenko, V., Mammarella, I., Ojala, A., Miettinen, H., Lykosov, V., & Vesala, T. (2016). Lake 2.0: A model for temperature, methane, carbon dioxide and oxygen dynamics in lakes. *Geoscientific Model Development*, 9(5), 1977–2006. <https://doi.org/10.5194/gmd-9-1977-2016>
- Tan, Z., Zhuang, Q., & Anthony, K. W. (2015). Modeling methane emissions from arctic lakes: Model development and site-level study. *Journal of Advances in Modeling Earth Systems*, 7(2), 459–483. <https://doi.org/10.1002/2014MS000344>
- Tranvik, L. J., Downing, J. A., Cortner, J. B., Loiselle, S. A., Striegl, R. G., Ballatore, T. J., et al. (2009). Lakes and reservoirs as regulators of carbon cycling and climate. *Limnology and Oceanography*, 54(6part2), 2298–2314. https://doi.org/10.4319/lno.2009.54.6_part_2.2298
- West, W. E., Coloso, J. J., & Jones, S. E. (2012). Effects of algal and terrestrial carbon on methane production rates and methanogen community structure in a temperate lake sediment. *Freshwater Biology*, 57(5), 949–955. <https://doi.org/10.1111/j.1365-2427.2012.02755.x>
- Whiticar, M. J., & Faber, E. (1986). Methane oxidation in sediment and water column environments—isotope evidence. *Organic Geochemistry*, 10(4–6), 759–768. [https://doi.org/10.1016/S0146-6380\(86\)80013-4](https://doi.org/10.1016/S0146-6380(86)80013-4)
- Wilkinson, J., Maeck, A., Alshboul, Z., & Lorke, A. (2015). Continuous seasonal river ebullition measurements linked to sediment methane formation. *Environmental Science and Technology*, 49(22), 13121–13129. <https://doi.org/10.1021/acs.est.5b01525>

- Yao, H., Conrad, R., Wassmann, R., & Neue, H. U. (1999). Effect of soil characteristics on sequential reduction and methane production in sixteen rice paddy soils from China, the Philippines, and Italy. *Biogeochemistry*, 47(3), 269–295. <https://doi.org/10.1007/BF00992910>
- Yvon-Durocher, G., Allen, A. P., Bastviken, D., Conrad, R., Gudas, C., St-Pierre, A., et al. (2014). Methane fluxes show consistent temperature dependence across microbial to ecosystem scales. *Nature*, 507(7493), 488–491. <https://doi.org/10.1038/nature13164>

References From the Supporting Information

- Cleveland, W. S., Grosse, E., & Shyu, W. M. (1992). Local regression models. In J. M. Chambers, & T. J. Hastie (Eds.), *Statistical models in S*. Wadsworth & Brooks/Cole.
- Pinheiro, J., & Bates, D., & R Core Team. (2023). nlme: Linear and nonlinear mixed effects models. R package version 3.1-162. Retrieved from <https://CRAN.R-project.org/package=nlme>